International Journal of Multiphysics
Volume 18, No. 2, 2024
ISSN: 1750-9548

High Temperature Performance Data Analysis and Evaluation of Quartz Crystal Resonators

Jia Liu, Hang Gu*, Fangmei Liu, Zuhe Li

School of Computer Science and Technology, Zhengzhou University of Light Industry, Zhengzhou 450002, China

*Corresponding Author.

Abstract

In recent years, with the continuous advancement of science and technology, quartz crystals have been playing an increasingly significant role in various fields. Particularly in the realms of computing and electronics, quartz crystals, as vital oscillatory components, have garnered considerable attention due to their stability and performance. This study used computer modeling simulation to investigate the vibration state of AT-cut quartz crystal resonators under different temperature conditions. Using the incremental thermal field equations, we established a mathematical model that correlates the elastic constants, piezoelectric coefficients, and dielectric constants with temperature. Using COMSOL Multiphysics finite element simulation software, we analyzed the displacement distribution in the X-direction of AT-cut quartz crystals under free vibration conditions at various temperatures. Additionally, the study examined the displacement distribution of spurious modes in the Y and Z directions. Subsequently, we introduced an energy distribution formula to calculate the energy proportion within the electrode area at different temperatures. The computer simulation data results show that with the increase of temperature, the surface displacement of the quartz crystal shows a typical energy capture phenomenon. Despite a slight decrease in energy proportion within the electrode area, the reduction is minimal, ensuring robust thickness shear vibration mode maintenance. This suggests that quartz crystals exhibit strong thermal stability in high-temperature environments, making them suitable as sensitive elements in Quartz Crystal Microbalance (QCM) sensors under such conditions.

Keywords: AT-cut, high temperature, COMSOL multiphysics, data analysis.

1. Introduction

In the industrial sector, humidity sensors are crucial and widely used in numerous fields. With the advancement of computer technology, the design and optimization of humidity sensors are increasingly reliant on computer simulation and data analysis methods[1,2]. Such as chemical gas purification, transformer oil health monitoring, semiconductor wafer processing, and paper and textile production[3,4]. When it comes to humidity assessment techniques, dew point measurement stands out as notably precise. Presently, the primary techniques employed for dew point detection arepredominantly based on Surface Acoustic Wave (SAW) technology and Quartz Crystal Microbalance (QCM) systems[5]. QCM offers significant advantages over other methodologies, including high stability and sensitivity to nanogram-level mass changes[6,7]. As a sensor, QCM is widely used to detect mass load changes by measuring variations in resonant frequency[8].

Quartz piezoelectric sensors are produced by leveraging the piezoelectric effect of quartz crystals to convert and transmit signals[9]. Their simple structure, high sensitivity, and real-time online monitoring capabilities make quartz piezoelectric sensors highly versatile with broad application prospects across various domains[10,11]. In the design of quartz piezoelectric sensors, AT-cut quartz crystal resonators are favored due to their excellent

characteristics and mature design and manufacturing techniques[12]. These features render them an optimal choice for robust and efficient sensor applications.

In recent times, numerous researchers have conducted extensive studies on the characteristics of QCM. Oigawa et al. developed a novel method that reshapes AT-cut quartz resonators into a plano-convex design with surface protrusions, enhancing quality factor and frequency stability, and boosting performance efficiency[13]. He and Yang refined previous perturbation methodologies, introducing accurate computations of natural vibration frequencies and patterns in round AT-cut quartz wafers, encompassing both thickness-shear and thickness-twist oscillation modes[14]. Furthermore, Huang and Ma used a variety of techniques to explore the forced vibration characteristics of these plates, enabling them to capture resonant frequencies and mode shapes in real time[15]. Additional researchers have explored the impact of temperature on quartz resonators' characteristics. Goka et al. designed and produced AT-cut quartz resonators with a tiered bi-mesa structure, subsequently characterizing their frequency response as a function of temperature[16]. Patel and Sinha performed a theoretical exploration using the three-dimensional finite element method (FEM) to investigate how high temperature affects the oscillation rates and Q factors of slow (C-mode) and fast (B-mode) thickness shear resonances in differently cut and AT-cut quartz crystals[17].

The outstanding frequency-temperature characteristics, wide frequency coverage, and mature design and manufacturing technology of AT-cut quartz crystal resonators have led to their widespread use in quartz resonator sensor design[18,19]. Existing QCM humidity sensors primarily operate in normal temperature environments, with limited research focused on high-temperature contexts. Given that quartz crystal, the sensitive element in QCM humidity sensors, is an anisotropic material significantly influenced by temperature, researching its physical properties in high-temperature environments is valuable. Investigating the vibrational characteristics of quartz crystal at various temperatures forms the foundation for using QCM sensors in high-temperature scenarios. This study employs the COMSOL Multiphysics simulation platform to conduct finite element analyses, focusing on examining the thickness-shear wave vibrational properties of AT-cut quartz crystal-based resonator devices under a range of thermal conditions. The objective is to ascertain the stability and dependability of quartz crystals when utilized as sensing components in Quartz Crystal Microbalance (QCM) humidity sensors operating under elevated temperature scenarios. Vibration modes and displacement distribution of AT-cut quartz crystal at various temperatures were determined, facilitating an intuitive analysis of its vibrational characteristics. Concurrently, the energy distribution across the crystal's surface electrode zones at assorted temperatures was assessed, validating its robust performance under high-temperature regimes. The software installation version is COMSOL Multiphysics 6.0, installed on Windows 10 Professional Edition.

2. Quartz Crystal Physical Parameter - Temperature Coefficient

Due to its piezoelectric properties and stable resonant frequency, quartz crystal is widely used in precision equipment. Both AT-cut and SC-cut quartz crystal configurations display fundamental relationships between temperature fluctuations and resultant frequency shifts. The AT-cut crystal is specifically cut at an angle of 35°15' relative to the crystallographic axis, while the SC-cut crystal is cut at various angles for applications requiring lower temperature sensitivity. The performance of these crystals at different temperatures is primarily attributed to changes in physical properties such as elastic modulus (Y) and density (ρ). The linear expansion coefficient of quartz crystal at room temperature is generally around 5.5*10-7. As the temperature increases, the elastic modulus of quartz decreases, leading to a reduction in the mechanical resonant frequency of the crystal. This phenomenon can be qualitatively expressed through the subsequent equation:

$$f = \frac{1}{2L}\sqrt{\frac{Y}{\rho}} \tag{1}$$

Here, L is the length of the crystal, $Y(T)$ is the temperature-dependent elastic modulus, and $\rho(T)$ is the density, which also varies with temperature.

The frequency constants of a specific quartz crystal cut are determined by parameters like size, density, and elastic constants. Simultaneously, the size, density, and elastic constants of the quartz crystal are affected by

temperature. Therefore, the characteristic frequency of the quartz crystal is affected by temperature. The constitutive relation equation for the quartz crystal is as follows:

$$T = C_E S - e^{\mathrm{T}} E \tag{2}$$

$$D = eS + \varepsilon_s E \tag{3}$$

Where T, S, E, D, $\boldsymbol{C_E}$, e, and ε_s represent stress, strain, electric field, electric displacement, elastic matrix, coupling matrix, and dielectric matrix, respectively. The material properties of the crystal are temperature dependent and can be expressed using a third-order polynomial as[20]:

$$e' = e_{ij}\left(1 + T_{e_{ij}}^{(1)}(T - T_0)\right) \tag{4}$$

$$\varepsilon^{\mathrm{T}} = \varepsilon_0{}^{\mathrm{T}}\left(1 + T_{\varepsilon^{\mathrm{T}}}^{(1)}(T - T_0)\right) \tag{5}$$

$$c_{ij}^{'} = c_{ij}(1 + T_{c_{ij}}^{(1)}(T - T_0) + T_{c_{ij}}^{(2)}(T - T_0)^2 + T_{c_{ij}}^{(3)}(T - T_0)^3) \tag{6}$$

The formula includes the reference temperature T_0 of 25°C, c_{ij} represents the elastic stiffness coefficients, e_{ij} represents the piezoelectric stress constants, and ε^{T} represents the dielectric constants. Under the reference temperature condition, the quartz crystal is considered to be in its inherent, unaltered material state, and in the uniform temperature field T_0, the crystal does not produce displacement, stress, or strain.

In 1986, Lee and Yong developed a series of linear equations to analyze the tiny vibrations superimposed on thermal deformations under uniform temperature changes by integrating the thermoelastic nonlinear field equations in a Lagrangian framework. This study is based on Lee's incremental thermal field theory and explores the subtle vibration behavior of quartz crystals under the influence of heat with reference to the properties of quartz crystals at 25°C. For example, for an AT-cut quartz crystal resonator operating at 70°C, the elastic stiffness, dimensions, piezoelectric and dielectric properties of the crystal at 70°C can be calculated using the incremental thermal field equations given the parameters at 25°C. In this context, the analysis focuses on the effect of temperature on the elastic matrix, coupling matrix and relative dielectric constant of the quartz crystal. The elastic temperature coefficients of quartz crystals are shown in Table 1:

Table 1 Elastic temperature coefficient at 25℃.

ij	$Tc_{ij}^{(1)}$ $(\times 10^{-6}/℃)$	$Tc_{ij}^{(2)}$ $(\times 10^{-9}/(℃)^2)$	$Tc_{ij}^{(3)}$ $(\times 10^{-12}/(℃)^3)$
11	-48.5	-107	-70
33	-160	-275	-250
22	-3000	-3050	-1260
13	-550	-1150	-750
44	-177	-216	-216
66	178	118	21
14	101	-48	-590

Table 2 Temperature coefficient of Y-cut piezoelectric constant at 25℃.

c	$e'^{(1)}_{ij}(\times 10^{-6}C/m^2/K)$	$e'^{(2)}_{ij}(\times 10^{-9}C/m^2/K^2)$	$e'^{(3)}_{ij}(\times 10^{-12}C/m^2/K^3)$
11	-1.370	-0.749	1.955
33	3.124	2.600	-4.692

Table 2 presents the temperature coefficients of the Y-cut piezoelectric constant of quartz crystals at 25°C. The relationship between the piezoelectric constant and the dielectric constant in quartz crystals can be explained through the crystal's elastic properties and polarization characteristics.

At 25°C, the temperature coefficients of the dielectric constant for a Y-cut type are respectively $\varepsilon_{11}^{\prime(1)}$=1.59020、$\varepsilon_{11}^{\prime(2)}$=5.37230、$\varepsilon_{11}^{\prime(3)}$=5.105736、$\varepsilon_{33}^{\prime(1)}$=5.46123、$\varepsilon_{33}^{\prime(2)}$=0.1894809、$\varepsilon_{33}^{\prime(3)}$=-9.230945[21]. The temperature coefficient matrix of piezoelectric constants for AT-cut can be obtained through Bond the coordinate transformation method.

In COMSOL MULTIPHYSICS software, the quartz crystal's elastic matrix, relative dielectric constant matrix, and coupling matrix are configured as functions of temperature. By specifying the surface temperature, the vibration state at various temperatures can be analyzed.

3. Finite Element Simulation

3.1 Establishment of quartz crystal resonator model

This study employs an AT-cut quartz crystal characterized by a diameter of 8.6 mm, thickness of 0.416 mm, and a cut angle of 35°15'. When configuring parameters, if the electrode thickness is under 50 nm, the mass load is insufficient to trigger energy trapping effects; conversely, excessively thick electrodes lead to increased energy dissipation and a reduction in the quality factor. This research applies gold electrodes, measuring 5 millimeters in diameter and 2 micrometers thick, to the opposing circular facets of the quartz crystal. The objective is to meticulously calibrate the interplay between energy confinement and dissipation, ensuring the preservation of a superior quality factor. The selected piezoelectric material is Quartz LH, with modifications to the elastic matrix, relative dielectric constant, and coupling matrix parameters based on the quartz crystal material's temperature-dependent analytical expressions. These adjustments ensure that the resonator's performance remains stable across a wide range of temperatures.

After a 0.1 V voltage difference is applied across the electrodes, the model integrates multiple physical fields, including solid mechanics, electrostatics, and solid heat transfer. To simplify the model, an isotropic mechanical loss of 1.1e-5 is incorporated into the solid mechanics field, and electrode heating loss is ignored. Additionally, the quartz crystal's surface temperature is specifically set using the temperature submodule in the solid heat transfer module.

The finite element geometric model of the AT-cut quartz crystal is depicted in Figure 1, where the central blue circle represents the electrode area, and the surrounding gray annulus denotes the bulk of the crystal. To ensure high degrees of freedom and accurate simulation results, Figure 2 il-lustrates the mesh structure optimized for computational efficiency and precision, with a total degree of freedom count of 104,227. The quartz crystal is not subjected to any mechanical constraints and is in a state of free vibration, making it ideal for assessing natural vibrational characteristics. The frequency scan range is set from 3.98 MHz to 4.01 MHz, with a step size of 0.1 kHz, to accurately determine the resonance frequency peak and its temperature dependence.

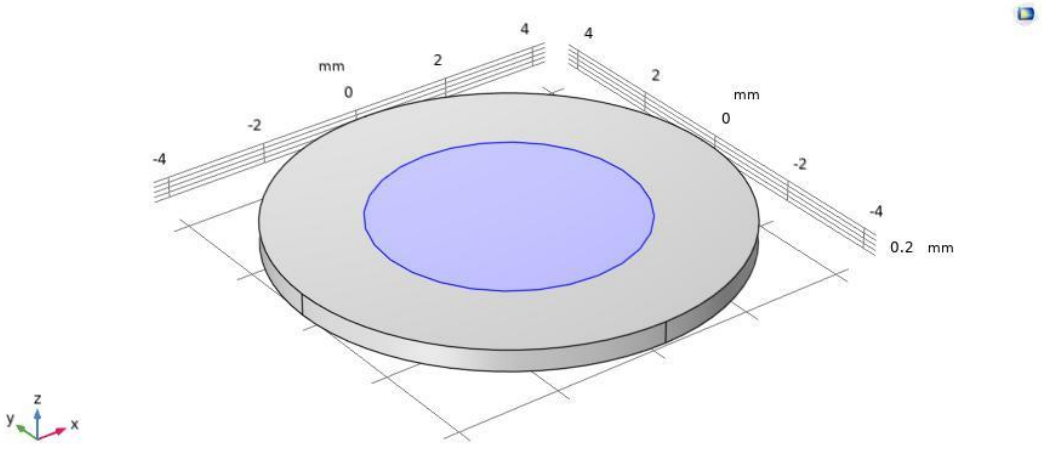

Figure 1 Geometric model of quartz crystal

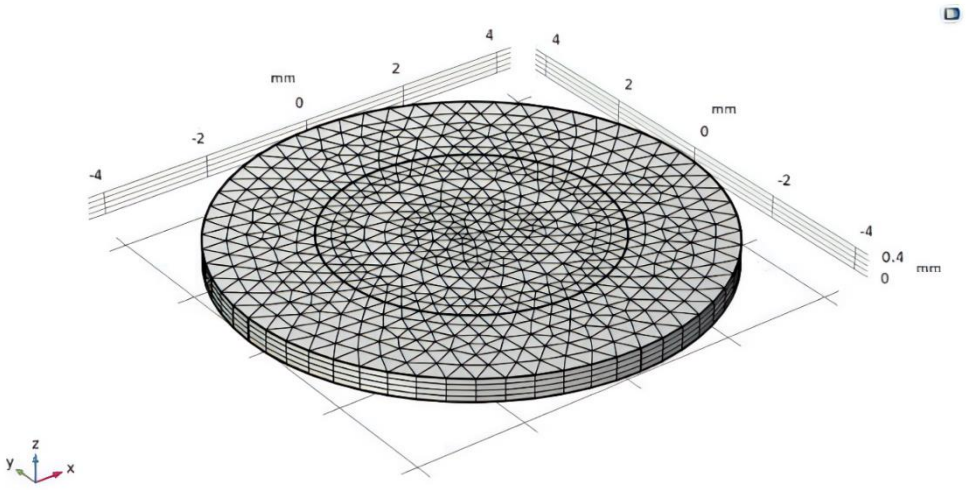

Figure 2 Quartz crystal meshing

3.2 Temperature effect on the vibrational characteristics of quartz crystals

This study performed finite element analyses on quartz crystals at environmental temperatures of 40°C, 90°C, 110°C, 130°C, and 150°C. Each analysis focused on demonstrating how temperature influences the vibrational characteristics of quartz crystals, particularly the thickness-shear vibration displacements on the crystal sur-face at different temperatures. The distribution of these displacements is visually depicted in the contour plot in Figure 3, illustrating the variations and intensities of sur-face vibrations across the temperatures examined.

The distribution in Figure 4 shows the displacement in different directions along the tangent line of the x-axis of the quartz crystal under five temperature conditions. The horizontal axis represents the position coordinates along the radial tangent of the quartz crystal, providing a detailed mapping of the displacement changes at a specific point. The vertical axis shows the magnitude of the thickness shear vibration dis-placement at any given point along the line, showing the spatial distribution of mechanical stress and its effect on temperature changes.

Figure 3 clearly demonstrates that, across various environmental temperatures, the surface vibration displacements of the quartz crystals are primarily concentrated within the electrode area, with rapid attenuation occurring outside this region. This displays a pronounced energy trapping phenomenon. Such an effect indicates that within the electrode area, the quartz crystal effectively confines vibrational energy, minimizing energy dissipation outward and thus enhancing the overall vibrational efficiency and the sensor's responsiveness. As the temperature increases, despite harsher environmental conditions, the vibration displacements on the quartz crystal surface remain localized to the electrode area with minimal temperature influence, showcasing the excellent thermal stability of AT-cut quartz crystals under high temperatures. This stability makes AT-cut quartz crystals highly suitable as sensitive components in QCM sensors, particularly in high-temperature environments, significantly enhancing the sensor's stability and reliability.

As the core element of QCM sensors, the thermal stability and energy trapping capability of AT-cut quartz crystals are crucial for sensor performance. In high-temperature environments, sensor performance often suffers due to material thermal expansion and other heat-related factors. However, the good thermal stability of AT-cut quartz crystals effectively mitigates these effects. Therefore, QCM sensors utilizing AT-cut quartz crystals offer higher reliability and stability in high-temperature applications, providing more precise measurements.

In the design of AT-cut quartz crystals, thickness shear vibration is the desired mode because it offers high frequency stability and precise control, which are crucial for applications in high-temperature environments. Therefore, displacements caused by parasitic modes, which usually induce unintended vibrations and energy losses, reducing the overall performance of the device, should be minimized. In Figure 4, the vibrations along the X direction are clearly due to the thickness shear mode, while dis-placements along the Y and Z directions are mainly caused by parasitic modes. More-over, the data from Figure 4 indicate that within the electrode area,

the displacement along the X direction is consistently higher than those along the Y and Z directions across various temperatures, suggesting that the thickness shear mode is dominant, although there is still some coupling between the parasitic and thickness shear modes.

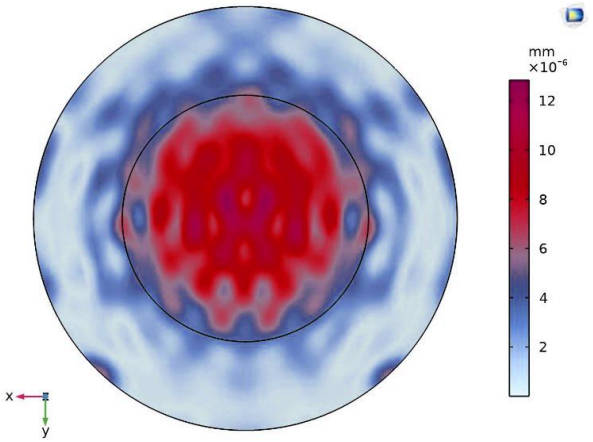

(a) 40℃, 3.9985MHz

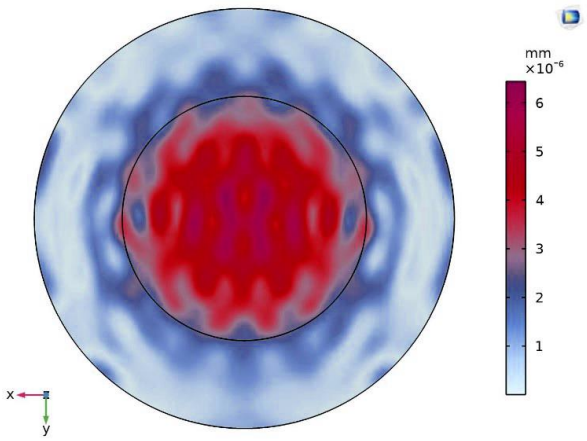

(b) 90℃, 3.9964MHz

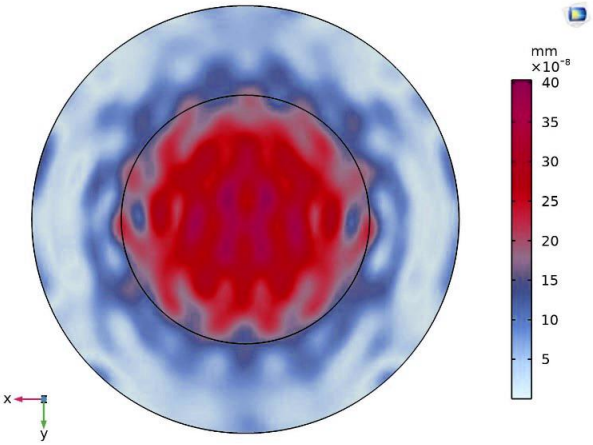

(c) 110℃, 3.9957MHz

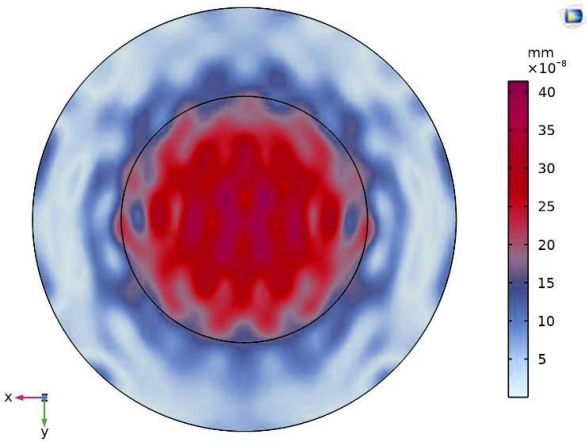

(d) 130℃, 3.9949MHz

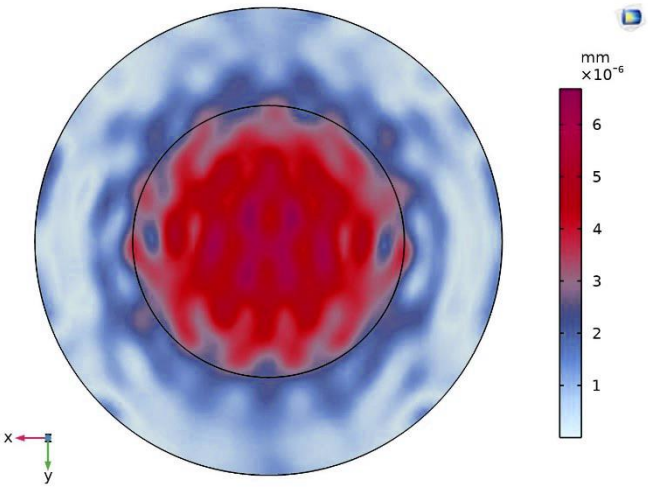

(e) 150℃,3.9943MHz

Figure 3 Thickness shear displacement distribution cloud map at different temperatures

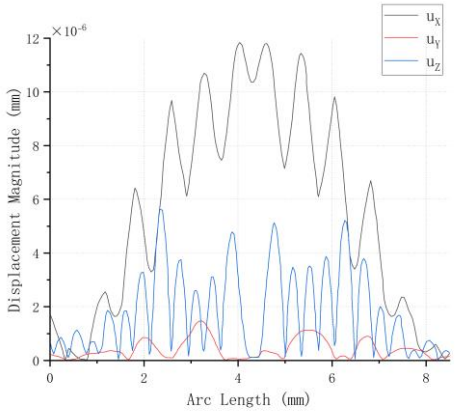

(a) 40℃

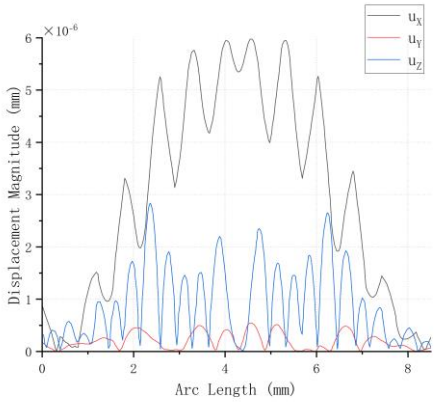

(b) 90℃

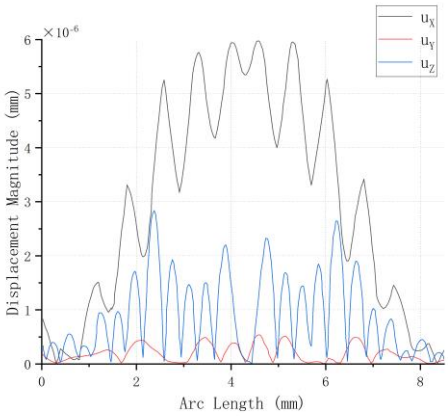

(c) 110℃

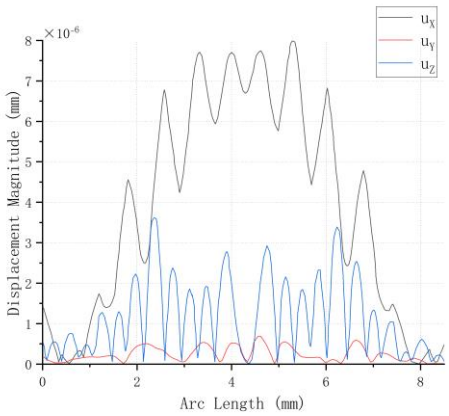

(d) 130℃

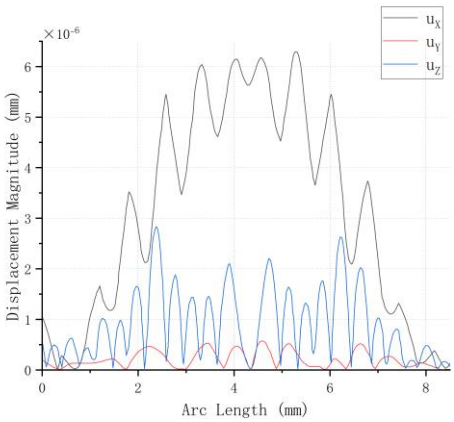

(e) 150℃

Figure 4 Displacement distribution along the radial line of X axis at different temperatures

Overall, despite the coupling, the amplitude of the thickness shear vibration is significantly higher than that of the parasitic mode, and this property shows good consistency at different temperatures, with little change with temperature. This once again proves that AT-cut quartz crystal has excellent thermal stability in high-temperature environments.

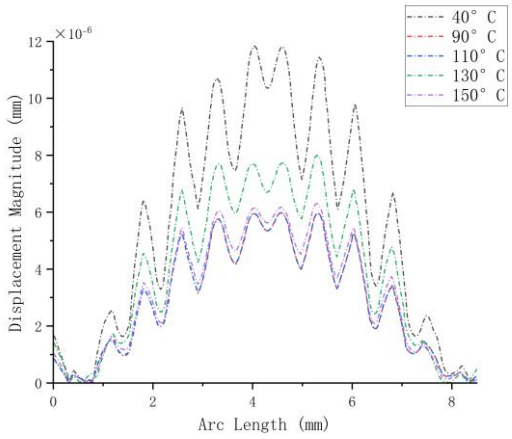

(a) X direction displacement

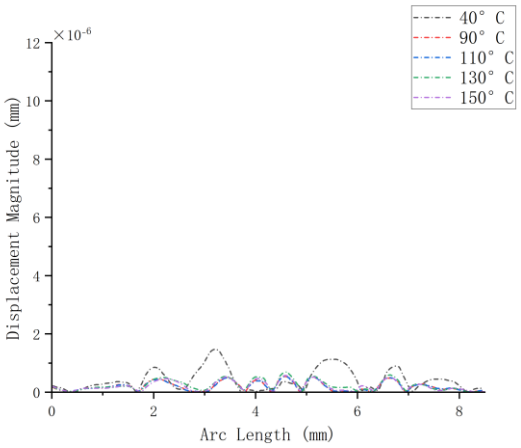

(b) Y direction displacement

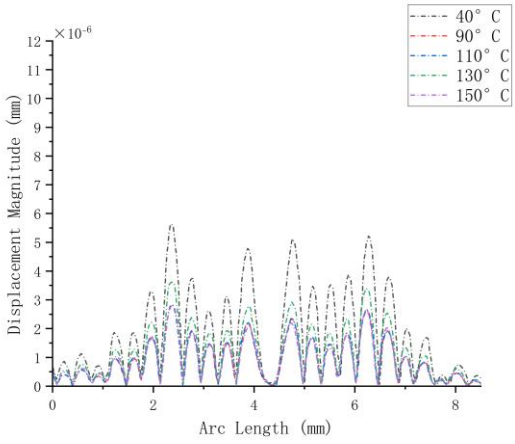

(c) Z direction displacement

Figure 5 Comparison of displacement amplitudes in X, Y and Z direction at different temperatures

Figure 5 reveals that with rising temperatures, the displacement along the X direction does not follow a distinct pattern. However, the vibration displacement continues to be localized within the electrode region. The amplitude of displacement undergoes significant variations with temperature, yet the overall trend of displacement change remains consistent, illustrating a characteristic energy limiting effect.

In the realm of quartz crystal resonator design, a paramount consideration is the vibrational stability, encapsulated prominently by the quality factor (Q). This parameter holds particular significance as it serves as a gauge for energy dissipation within vibratory systems, fundamentally shaping the resonator's functional efficacy. The quality factor is calculated using the following formula:

$$Q = \frac{1}{4\pi RC\Delta f} \tag{7}$$

Where R represents the equivalent resistance of the quartz crystal, C denotes the equivalent static capacitance, and Δf indicates the change in frequency. These parameters are calculated using the following formula:

$$R = \frac{d^3 r}{8Ae_{26}} \tag{8}$$

$$C = \frac{\varepsilon_{22} A}{d} \tag{9}$$

Here, d signifies the crystal's thickness dimension, whereas A indicates the extent of the electrode area. ε_{22} is the dielectric constant, e_{26} is the electromechanical coupling coefficient. Besides r is damping coefficient. In this study, the following parameter values are used: d =0.416 mm, A =4.91×10−6 m², e_{26} =9.65×10−2 C·m², ε_{22} =39.82×10−12 C·V^{-1}·m^{-1}, r =1.45×10^{-7}.

Using finite element software simulation, we directly calculated the quality factor (Q) of the quartz crystal. As illustrated in Table 3 below, the temperature conditions analyzed are 40°C, 90°C, 110°C, 130°C, and 150°C. Temperature increments are 50°C and 20°C. Changes in quality factors are -13, -16, +5, and +9. This data demonstrates that the quality factor of the AT-cut quartz crystal remains relatively stable with temperature changes, confirming its excellent thermal stability in high-temperature environments.

Table 3 Quality factor changes in AT-cut quartz crystal with temperature.

Temperature (°C)	Temperature Change (°C)	Quality Factor (Q)	Change in Quality Factor (Compared to Previous)
40	—	68,789	—
90	+50	68,776	-13
110	+20	68,760	-16
130	+20	68,765	+5
150	+20	68,756	-9

To accurately measure the vibration displacement on AT-cut quartz crystal surfaces at various temperatures, we introduced an energy distribution calculation formula specific to the electrode region[22]. This method calculates the energy proportion within the electrode region of the quartz crystal at different temperatures by comparing the integral of displacement amplitude in the X direction inside the electrode area with the total displacement integral across the quartz crystal surface along the X axis.

$$E_r = \frac{\iint_{r<\frac{d_r}{2}} (u_X^2 + u_Y^2 + u_Z^2) dxdy}{\iint_{r<\frac{d_q}{2}} (u_X^2 + u_Y^2 + u_Z^2) dxdy} \tag{10}$$

d_r and d_q respectively represent the diameters of the electrode area and the quartz crystal, and u_x denotes the displacement of the quartz crystal surface along the X direction. The energy distribution across the quartz crystal's surface was computed for temperatures reaching 40°C, 90°C, 110°C, 130°C, and 150°C, with the results depicted in Figure 6. The horizontal axis of the graph shows the temperature range of the quartz crystal, and the vertical axis shows the ratio of the thickness shear displacement occurring in the electrode region to the total surface displacement of the crystal.

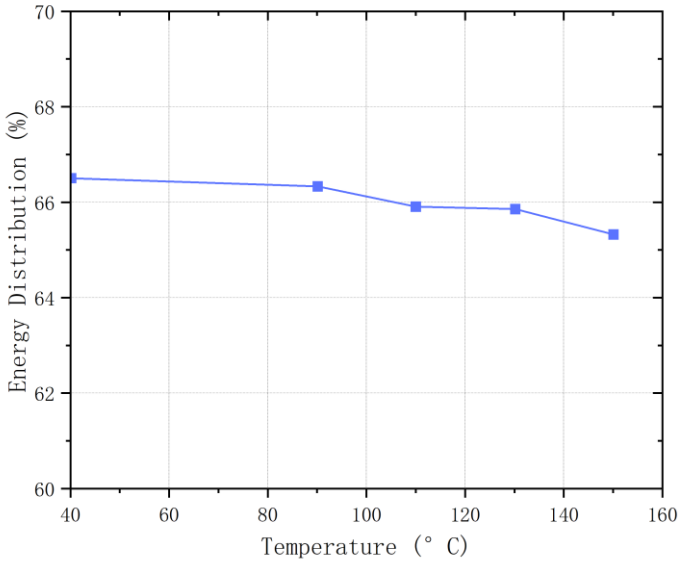

Figure 6 Quartz crystal electrode area energy ratio

As illustrated in Figure 6, the energy proportion in the electrode area of the quartz crystal surface decreases as the temperature rises. At 40°C, the energy proportion is 66.2%, which drops to 65.34% at 150°C. Although there is a slight reduction, the overall change is minimal, indicating that the energy distribution remains relatively stable even in high-temperature environments. This stability underscores that AT-cut quartz crystals, as sensitive elements of QCM humidity sensors, can maintain the stability and reliability of the sensors under high temperatures.

This thermal stability is particularly critical in industrial and scientific research sectors where sensors frequently operate in unstable or harsh environments. By ensuring reliable data output under such conditions, the unique properties of AT-cut quartz crystals significantly enhance the overall quality and performance of the sensor products. Additionally, this also highlights the high quality and adaptability of AT-cut quartz crystals in their design, making them an indispensable material for various high-temperature applications.

4. Conclusion

In this study, the geometric model of AT-cut quartz crystal resonator was established by finite element analysis. The displacement change of the AT-cut resonator crystal surface along the X direction at different temperatures was further simulated. This study aimed to understand the effect of high temperatures on quartz crystal thickness shear vibrations, which is critical for the operational stability of QCM humidity sensors under such conditions. The results show that the modal coupling and energy trapping effects of the quartz crystal have no effect under all tested temperature changes. The vibrational displacement distribution remains localized within the electrode region, which demonstrates the strong thermal stability of the crystal. This stability is critical to maintaining sensor accuracy and reliability in high-temperature environments. And based on the quality factors at different temperatures, it shows that AT-cut quartz crystal has good thermal stability in high-temperature environments. The results demonstrate the suitability of AT-cut quartz crystals as sensitive elements in QCM sensors operating at high temperatures and illustrate their potential to maintain stability and reliability under harsh thermal conditions. Future research should further explore the integration of these vibration characteristics into sensor de-signs to improve their efficiency and operating range in industrial applications.

Acknowledgment

This research has received support from the Henan Provincial Science and Technology Research Project under Grant 222102210304, the National Defense Basic Research Project (Project Number JCKY2021601B011).

References

[1] S. K. Baduge et al., "Artificial intelligence and smart vision for building and construction 4.0: Machine and deep learning methods and applications," Automation in Construction, vol. 141, p. 104440, 2022.
[2] C. Yang, Q. Huang, Z. Li, K. Liu, and F. Hu, "Big Data and cloud computing: innovation opportunities and challenges," International Journal of Digital Earth, vol. 10, no. 1, pp. 13-53, 2017.
[3] Z. Wang, H. Zhu, Y. Dong, and G. Feng, "A temperature insensitive quartz resonator force sensor," Measurement Science and Technology, vol. 11, no. 11, p. 1565, 2000.
[4] M. Hopcroft et al., "Using the temperature dependence of resonator quality factor as a thermometer," Applied physics letters, vol. 91, no. 1, 2007.
[5] R. Melamud et al., "Temperature-insensitive composite micromechanical resonators," Journal of Microelectromechanical Systems, vol. 18, no. 6, pp. 1409-1419, 2009.
[6] B. Liu et al., "Surface acoustic wave devices for sensor applications," Journal of semiconductors, vol. 37, no. 2, p. 021001, 2016.
[7] J. Kankare, "Sauerbrey equation of quartz crystal microbalance in liquid medium," Langmuir, vol. 18, no. 18, pp. 7092-7094, 2002.
[8] H. Nanto et al., "A smart gas sensor using polymer-film-coated quartz resonator microbalance," Sensors and Actuators B: Chemical, vol. 66, no. 1-3, pp. 16-18, 2000.
[9] Y. Saigusa, "Quartz-based piezoelectric materials," in Advanced Piezoelectric Materials: Elsevier, 2017, pp. 197-233.
[10] R. Abdolvand, H. Fatemi, and S. Moradian, "Quality factor and coupling in piezoelectric mems resonators," Piezoelectric MEMS Resonators, pp. 133-152, 2017.
[11] G. Pillai and S.-S. Li, "Piezoelectric MEMS resonators: A review," IEEE Sensors Journal, vol. 21, no. 11, pp. 12589-12605, 2020.
[12] G. Piazza, "Piezoelectric resonant MEMS," Resonant MEMS: Fundamentals, Implementation and Application, pp. 147-172, 2015.
[13] H. Oigawa, Y. Sakano, J. Ji, D. Yamazaki, and T. Ueda, "Vibration analysis of original shape quartz resonator for high Quality factor realization," Japanese Journal of Applied Physics, vol. 51, no. 6S, p. 06FL02, 2012.
[14] H. He, J. Yang, and Q. Jiang, "Thickness-shear and thickness-twist vibrations of circular AT-cut quartz resonators," Acta Mechanica Solida Sinica, vol. 26, no. 3, pp. 245-254, 2013.
[15] Y.-H. Huang and C.-C. Ma, "Forced vibration analysis of piezoelectric quartz plates in resonance," Sensors and Actuators A: Physical, vol. 149, no. 2, pp. 320-330, 2009.
[16] S. Goka, H. Sekimoto, Y. Watanabe, and T. Sato, "Frequency-temperature behavior of stepped bi-mesa-shaped AT-cut quartz resonators," Japanese journal of applied physics, vol. 41, no. 5S, p. 3450, 2002.
[17] M. S. Patel and B. K. Sinha, "Frequency-temperature (fT) behavior for different rotated quartz cuts at high temperatures and their Q-factor estimation," in 2010 IEEE International Ultrasonics Symposium, 2010: IEEE, pp. 400-403.
[18] Y.-K. Yong, M. Patel, and M. Tanaka, "Effects of thermal stresses on the frequency-temperature behavior of piezoelectric resonators," Journal of Thermal Stresses, vol. 30, no. 6, pp. 639-661, 2007.
[19] P. Luo, J. Yuan, and X. Shan, "The analysis of harmonic frequency of AT-cut disc-typed quartz crystals resonator," in AIP Conference Proceedings, 2017, vol. 1834, no. 1: AIP Publishing.
[20] P. Lee and Y. Yong, "Frequency-temperature behavior of thickness vibrations of doubly rotated quartz plates affected by plate dimensions and orientations," Journal of Applied Physics, vol. 60, no. 7, pp. 2327-2342, 1986.
[21] M. Li et al., "The multi-field coupled vibration analysis of AT-cut quartz crystal resonators with parallelism error," Acta Mechanica Solida Sinica, vol. 36, no. 2, pp. 349-360, 2023.
[22] N. Li, X. Meng, J. Nie, and L. Lin, "Structure optimization and performance evaluation of dew point sensors based on quartz crystal microbalance," IEEE Sensors Journal, vol. 18, no. 3, pp. 1016-1022, 2017.